A MODEL FOR THE LONG TIME-CONSTANT TRANSIENT VOLTAGE RESPONSE TO CURRENT IN EPITHELIAL TISSUES

GEORGE W. KIDDER III *and* W. S. REHM

From the Department of Physiology and Biophysics, University of Alabama in Birmingham, Birmingham, Alabama 35233. Dr. Kidder's permanent address is the Biology Department, Wesleyan University, Middletown, Connecticut 06457.

ABSTRACT Upon passing a step current through the frog gastric mucosa, a transient response in voltage is observed, which can formally be represented by several types of model systems, although some models require elements which are hard to visualize in terms of the known morphology of the mucosa. A physically reasonable model can be constructed by considering the changes in intracellular ionic composition which arise due to current flow, and the consequent changes in diffusion potentials across the two cell membranes. A simple model has been developed which fits the observed long time-constant portion of the transient at low current densities, and predicts departures from exponential behavior at larger currents. Since reasonable values for membrane resistance and cell volume give a fit, it is proposed that this model may account for the long time-constant portion of the transient response. There is no reason to expect that similar considerations do not hold for epithelial tissues in general.

INTRODUCTION

Since its introduction by Ussing and Zerahn in 1951, the short-circuit current technique has been widely used for measurements of active transport in epithelial tissues. Smaller currents, which do not reduce the potential difference (PD) to zero, have been used to measure tissue resistance (Rehm, 1943, 1953) while large currents, both hypo- and hyper-polarizing, have been employed to modify ion movements (Rehm, 1945, 1950, 1956, 1962 *a*; Crane and Davies, 1951; Curran and Cereijido, 1965). Thus, the subject of the interaction of current and voltage is of interest in the study of active transport processes in epithelial tissues.

If the tissue could be represented as a combination of fixed resistances and fixed emf's, there would be no problem. Application of direct current would lead to a step change in voltage which would be maintained at a constant level for the duration of the current flow. However, this state of affairs is not obtained in many tissues. For instance, Durbin and Heinz (1958) and others (Harris and Edelman,

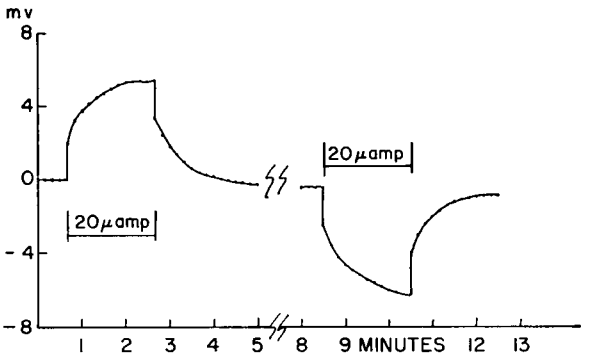

FIGURE 1 A typical long time-constant transient. Note initial step change followed by exponential curve, as current is sent for 180 sec, first in one direction and then in the other. Secreting gastric mucosa in Cl^- medium, histamine stimulated. The ordinate represents the potential minus the resting potential.

1964; Rehm, 1967) have observed that passage of small step currents across the isolated gastric mucosa of the frog results in a nonstep response in voltage. This phenomenon has been reported in other tissues (Ussing and Windhager, 1964; Cooperstein and Hogben, 1959) and seems to be typical of epithelial membranes.

Such a response is shown in Fig. 1. Rehm has analyzed the response of the gastric mucosa, and concluded that it behaves as if it were composed of a series of resistance-capacitance (*RC*) circuits with time constants ranging from a few milliseconds to about 35 sec. The analysis of the longest of these time constants (which can be recorded on conventional ink recorders) will be the subject of this paper. For our purposes we will define R_0, the DC resistance of the tissue, as the voltage change before the onset of the long time-constant transient, but after the shorter time-constant transients are over, divided by the current, I. Thus, our R_0 is equal to the R_i of Durbin and Heinz (1958).

At least three sorts of model systems can be used to represent the situation shown in Figure 1. These classes include models involving resistances and capacitors, models postulating resistances which vary with current, and models postulating changes in emf's due to shifting ionic concentrations. There are, of course, combinations of these classes. The choice of model is of some importance, as it affects the meanings of the electrical parameters. For instance, if one believes that the *RC*-circuit model really exists in the tissue, then the DC resistance of the tissue must be measured after this capacitance has been charged, while if polarization emf's are responsible for the transient, the appropriate DC resistance is the short time value, before the emf's have started to change appreciably.

To consider the resistance-capacitance model, the time constant of an *RC* circuit, τ, is given by

$$\tau = RC, \tag{1}$$

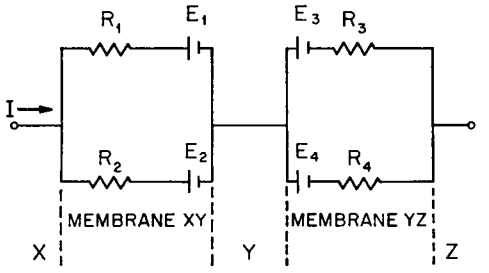

FIGURE 2 Electrical model for the long time-constant transient, with region Y representing the cell cytoplasm enclosed by membrane XY and YZ. R_1 and R_3 are cation-permeable regions, across which diffusion PD's E_1 and E_3 are developed; R_2 and R_4 are the corresponding anion-permeable regions. E_1 through E_4 are drawn in their positive orientation.

where the units are seconds, ohms, and farads. The measured time constant for the long time-constant transient in the frog gastric mucosa is about 25 sec. On the assumption that the long time-constant transient is due to an actual *RC* circuit, the value for R is about 100 ohm·cm^2 and C must therefore be about 0.25 farad/cm^2, which is absurdly high. Rehm (1967) has therefore concluded that this portion of the transient, while formally capable of representation by an *RC* circuit, is not actually a system involving a real membrane resistance and capacitance.

The variable-resistance model of Mauro (1961; Finkelstein and Mauro, 1963) is an example of the second type of model. The resistance and voltage changes predicted by these authors must certainly take place within the cell membranes, but there are a number of reasons to suspect that they cannot account for the long time-constant transient under discussion. Except for some quite special cases, this model would require that the "charge" and "discharge" responses would not be superimposable at low current densities, which is contrary to experimental findings (Rehm, 1967). Further, our data (presented below) do not show any changes in tissue resistance at low current densities, which again requires a rather special situation in the Mauro model. Finally, since the changes in concentrations involved in this model are supposed to take place within the membrane, it is difficult to imagine such slow changes within the very thin plasma membrane. This model may very well account for some of the faster transients observed in this tissue, but it would seem that an alternate model might be useful for the long time-constant transient under discussion.

A suitable model can be achieved by considering the changes in ionic concentration in a region between two membranes of different properties, a mechanism which can also act to store energy. Such a model is shown in Fig. 2, and is an extension of the model considered by Rehm (1968 *a* and *b*) with reference to the meaning of short-circuit current. For simplicity, we have deliberately excluded several complicating factors which are present in the real tissue. We will not consider H^+ transport at all; neither will we allow exchange diffusion or ion pair migration, and we will not consider the effect of the real membrane capacitances which are undoubtedly present. All of these factors, and others, such as combinations of this model with models of the other classes, could be introduced into the model at a later stage.

DEVELOPMENT OF THE MODEL

In this simple model, membrane XY represents one membrane of a sheet of cells, while membrane YZ is the other. The cell interior, Y, has a volume v, while the external bathing solutions, X and Z, have infinite volume. All compartments are well stirred, and the concentrations in all compartments are initially the same.

If we restrict ourselves to a single uni-univalent electrolyte, (say KCl), then R_1 and R_3 are the cation channels through the membranes, and R_2 and R_4 are anion channels. The separation of cation and anion channels implied by this statement is reasonable in light of the very high degree of specificity exhibited by biological membranes. In general, there is no a priori reason for assuming that these resistances are equal or related to one another in any systematic way. The E_i's are the diffusion potentials associated with ion permeabilities, and are initially zero, since there is no concentration difference between X, Y, and Z. (We exclude active transport for the time being.) We further assume no water movement, and that all activity coefficients are unity so that activities can be replaced by concentrations.

In the following discussion positive current is current flowing from X to Z and the voltages are given a positive sign when their left-hand side is positive.

Let a small step of current, I, pass through this system from X to Z. At time zero, just after the current starts, the voltage across the system is given by Ohm's law applied to the series-parallel combination of resistances. Thus, the resistance, R_0, is given by

$$R_0 = R_1R_2/(R_1 + R_2) + R_3R_4/(R_3 + R_4), \tag{2}$$

and the initial voltage step, V_0 is

$$V_0 = IR_0. \tag{3}$$

Since we wish to follow ion movements, we need to know the current through each resistor, as these currents are composed of moving ions. It is easily demonstrated that the current through a limb, say through R_2, is given by

$$I_2 = (E_1 - E_2)/(R_1 + R_2) + IR_1/(R_1 + R_2) \tag{4}$$

and similarly for R_4

$$I_4 = (E_3 - E_4)/(R_3 + R_4) + IR_3/(R_3 + R_4). \tag{5}$$

Similar expressions apply to the cation currents. At zero time these expressions contain only the last term since all E's are zero. Let us look at the anion current. In general, $R_1/(R_1 + R_2) \neq R_3/(R_3 + R_4)$, so $I_2 \neq I_4$ at zero time. Since these currents are anion fluxes, and represent the only means of anion entry and exit available to Y, it follows that the anion concentration at Y must change. Similar

arguments show that the cation concentration at Y changes by the same amount. This change in concentration will continue as long as the unbalance in currents continues. Eventually a steady state will obtain, in which the contributions of the first terms in equations 4 and 5 make the currents equal. This occurs because of the changes in the diffusion potentials (E's) set up by the concentration shift at Y.

We can write expressions for the voltage between X and Z, as

$$V = E_1 + I_1R_1 + E_3 + I_3R_3 = E_2 + I_2R_2 + E_4 + I_4R_4 . \tag{6}$$

These E's are calculated from the Nernst equations, for instance,

$$E_1 = (\mathrm{RT}/F) \ln ([\text{cation}]_Y/[\text{cation}]_X), \tag{7}$$

where R, T, and F have their usual meaning. If the concentrations at X and Z are equal, we can define an E, as

$$E = E_1 = -E_2 = -E_3 = E_4 , \tag{8}$$

and hence, the E's cancel in equation 6.

We can also arrive at an expression for V by eliminating the I's from equation 6 by means of equations 2, 4, 5, and 8, i.e.,

$$V = R_0 I + \frac{(R_2/R_1) - 1}{(R_2/R_1) + 1} E - \frac{(R_4/R_3) - 1}{(R_4/R_3) + 1} E. \tag{9}$$

This expression is valid for all times.

Since the steady state is defined as the state in which the concentration at Y is not changing, it follows that in this state $I_1 = I_3$ and $I_2 = I_4$. Since $I = I_1 + I_2$ at all times, we can arrive at an expression for the voltage in the steady state:

$$V_\infty = \frac{(R_1 + R_3)(R_2 + R_4)I}{R_1 + R_2 + R_3 + R_4}. \tag{10}$$

This gives rise to an apparent resistance (V_∞/I) which is larger than R_0, and is equal to the R_f of Durbin and Heinz (1958).[1]

The "magnitude" of the transient, V_∞/V_0, which is of interest in comparing

[1] This apparent resistance, R_∞, is what is measured by dividing the steady-state open circuit PD by short-circuit current (Hogben, 1955), or by measuring voltage changes after a long time, as apparently done by Crane, Davies, and Longmuir (1948) and Crane and Davies (1951). This will measure the resistance of the system only when $R_2/R_1 = R_4/R_3$; i.e., when there is no transient. In the general case, when $R_\infty > R_0$, for R_∞ to represent the true resistance, the circuit would have to be modified so that there would be two parallel limbs, one of which would be $R_1 + R_3$ and the other $R_2 + R_4$, with no connection between them in compartment Y. Proof that equation 10 gives the maximum value of V can be obtained from equation 8 A in Appendix A by letting $t \to \infty$, and then solving for V_∞ from the relation $V_\infty - V_0 = \Delta V_\infty$.

different tissues, is given by substituting equation 2 into 3 to obtain V_0 as a function of the R's and I and using this function to divide into equation 10 to obtain

$$\frac{V_\infty}{V_0} = \frac{\dfrac{(R_1 + R_3)(R_2 + R_4)}{R_1 + R_2 + R_3 + R_4}}{\dfrac{R_1 R_2}{R_1 + R_2} + \dfrac{R_3 R_4}{R_3 + R_4}}. \tag{11}$$

V_∞/V_0 is thus seen to be a function of the resistances alone, and can vary from 1 to some higher value. As can be seen from equations 9 and 11, when $R_2/R_1 = R_4/R_3$, V_∞/V_0 is unity, and there is no transient. Under these conditions the second and third terms in equation 9 cancel, and $V = V_0 = V_\infty = R_0 I$, and $V_\infty/V_0 = 1$ from equation 11. The smaller R_2/R_1, and the higher R_4/R_3, the greater will be the value of V_∞/V_0, and vice versa. In the limit, if $R_1 = \infty$ and $R_2 = 0$, then $V_\infty/V_0 = 1 + R_4/R_3$, and the observation of a transient of magnitude $V_\infty/V_0 = 3$ requires that R_4 be at least twice R_3. Conversely, if $R_1 \to 0$ while $R_2 = \infty$, the transient is given by $V_\infty/V_0 = 1 + R_3/R_4$.

For the period of time between time zero and the steady state, the voltage is given by a more complex expression, since $I_1 \neq I_3$, and $I_2 \neq I_4$, during this time. The differential equations relating the voltage change to these quantities are given as follows.

The rate of change of concentration at Y depends on the currents and the volume, and is

$$\frac{dC_Y}{dt} = \frac{d[\text{cation}]_Y}{dt} = \frac{d[\text{anion}]_Y}{dt} = \frac{I_4 - I_2}{Fv} = \frac{I_1 - I_3}{Fv}, \tag{12}$$

where F is the Faraday, and v is the volume of compartment Y. Focusing on the anion changes (and remembering that the cation changes are parallel), we have expressions for I_2 and I_4 (equations 4 and 5), which are given in terms of the value of E, as well as the R's and I.

Since the currents change the concentration at Y, which in turn determines the value of E, and E is part of the equations for I's, the calculation of the transmural potential at some intermediate time is rather complex. We have been able to arrive at analytical solutions for certain cases, and have resorted to an iterative solution, suitable for electronic computation, for a more general solution.

Combining equations 4, 5, 7, 8, and 12 gives rise to a differential equation relating the voltage change to time, which can be integrated to a converging series. (See Appendix A for details.) The first term of this solution contains the single entry of time and constants such as I, C_0, R's, and v. The subsequent terms contain V itself in addition, and thus the complete expression requires iterative calculation.

Using the first term, which is sufficiently accurate for small current densities, we

have

$$\Delta V = V - V_0 = \left[\frac{I(R_1R_4 - R_2R_3)^2}{(R_1 + R_2 + R_3 + R_4)(R_1 + R_2)(R_3 + R_4)}\right](1 - e^{-\theta t}), \quad (13)$$

in which θ is given by

$$\theta = \frac{2RT(R_1 + R_2 + R_3 + R_4)\exp\left[\dfrac{(R_1R_4 - R_2R_3)IF}{2RT(R_1 + R_2 + R_3 + R_4)}\right]}{F^2\nu C_0(R_1 + R_2)(R_3 + R_4)}, \quad (14)$$

where R is the gas constant, T the absolute temperature, $C_0 = C_X = C_Y$, and the other symbols are as before. Equation 13 applies to charging conditions (current on). Upon discharge (following the interruption of the current) the voltage, ΔV_D, is given by

$$\Delta V_D = \Delta V e^{-\theta' t}, \quad (15)$$

where ΔV is calculated from equation 13, or given by $\Delta V = V_\infty - V_0$ if the steady state has been obtained during the current-on period. The exponent θ' differs from θ of equation 14 only in that the exponential in its numerator is equal to unity, since $I = 0$. Since, in equation 14, the exponential term $\to 1$ as $I \to 0$, $\theta \to \theta'$ as $I \to 0$, and equation 13 is bilaterally symmetrical for low currents.

Equations 13 and 15 are single exponential functions in time, and, once the constants are calculated from the R's, I, F, ν, C_0, etc., are capable of solution. Since the long time-constant transient is essentially a single exponential at low currents, this equation can be made to fit by appropriate choice of resistances and volume.

Note the relationships in equation 14 between ν, the volume of the (intracellular) compartment Y, and C_0, the initial concentration of this compartment (which equals the concentration at X and Z, in the absence of any active transport). In the complete solution these constants appear only once and as a product; if C_0 is halved, then ν must be doubled to preserve the same constant. Physically, this is due to the fact that when C_0 is lowered, a smaller ionic movement will produce a given change in C_Y/C_0 than if C_0 is high; it is this ratio which determines the diffusion potential.

The solutions given in equations 13 and 15 are limited in several respects. They can deal only with equal concentrations at X and Z, with situations devoid of active transport (that is, where $C_Y = C_X = C_Z$ during the open-circuit steady state), and are valid only for currents sufficiently low that the later terms in the full expansion can be ignored.

The limitation that $C_X = C_Z$ can be removed (see Appendix B), but in integrating this system we make the assumption that the current is low enough that we can replace an expression of the form ln $(1 + x)$ by its approximate equivalent, x.

This leads to only a negligible error in the low current density ranges, since the actual magnitude of $V_\infty - V_0$ is only a millivolt or so. The solution is not applicable to the higher current density range when $V_\infty - V_0$ is greater than a few millivolts.[2]

Using the form given here, limited to $C_X = C_Z$, one can handle high currents by making use of the latter terms of the expansion, which would require iterative calculation, since these terms contain ΔV. We have chosen, therefore, to resort to a numerical integration method, which is perfectly general and allows a great deal of freedom in our choice of conditions.

For this solution, we use the same set of equations (4, 5, 7, 12) as before. Briefly, the scheme consists of selecting a short, finite time interval, Δt, and calculating the concentration change which would occur at Y during this interval, on the assumption that the E's and I's are not altered significantly during this period. Thus,

$$\Delta[\text{anion}]_Y = (\Delta t/F \cdot v)(I_4 - I_2), \tag{16}$$

where I_2 and I_4 are calculated according to equations 4 and 5, which are, in turn, calculated from E's derived from equations similar to equation 7. The concentrations used in equation 7 are those existing at the beginning of Δt, and the change in concentration calculated by equation 16 is added to the preexisting $[\text{anion}]_Y$ at the end of Δt, which establishes the conditions for the next loop. We have arbitrarily set limits on the amount by which $[\text{anion}]_Y$ is allowed to change in a single loop: if $\Delta[\text{anion}]_Y$ is larger than 0.1 % of $[\text{anion}]_Y$, the program reduces the value of Δt and recomputes. This limit is arbitrary, but is justified by the observation that the results are unchanged if the limit is increased to 1 %, and furthermore that with low current densities the results are indistinguishable from the results of equations 13–15. Therefore, we believe that the approximation used is a close one, and that I_4 and I_2 are not sensibly changed during any period Δt. The computer is allowed to operate for 3500 such increments in Δt, which ensures that the steady state has been attained.

With this program we can make several important modifications to our initial scheme. We can now include the effect of active transport in any limb by replacing the expression for the "battery" voltage (E_1, for instance) by a term E_1^A representing

[2] This approximation should not lead to large errors at the lower current densities. With 10 μamp/cm^2 when $A_Y = B_Y$ (see Fig. 7) the value of $\Delta C/B_0$ is about 0.07 and when $\Delta C/B_0$ (or $\Delta C/A_0$) is 0.10 or 0.20 the error is about 5% and 10% respectively. (The E's would be about 5 mv with $\Delta C/B_0 = 0.2$). E_∞ should be approximated by ΔV_∞ when values of the parameters consistent with the experimental findings are used. If the above approximation is not used integration involves the solution of an integral of the form

$$\int \frac{e^{-K_2 Y + K_3}\, dy}{(K_1 - 4e^{-K_2 y + K_3})^{1/2}(K_4 y - K_5)},$$

where the K's are constants and y corresponds to ΔV. We choose not to attempt this integration.

the active transport (see below). (Inclusion of active transport potentials renders equation 8 invalid; thus, this step is of necessity restricted to the computer solution.) We are also free to deal with unequal concentrations at X and Z, and we have ready access to intermediate values, such as C_Y, which are of interest.

EXPERIMENTAL METHODS

Frog (*Rana pipiens*) gastric mucosa, stripped of its external muscle layers, was mounted as a flat sheet (area 1.3 cm^2) between two fluid-filled chambers. The nutrient bathing solution contained, in millimoles per liter, Na^+ 102, K^+ 4, Ca^{++} 1.7, Mg^{++} 0.8, Cl^- 90, HCO_3^- 18, phosphate 1.0, and glucose 10. The secretory bathing solution contained the same cation concentrations, but with Cl^- as the only anion, and no glucose (Rehm, 1962 *a*, 1962 *b*). Continuous measurements of transepithelial PD, and H^+ secretory rate were obtained with a recording potentiometer and a recording pH-stat. Resistance (R_0) measurements were obtained by automatically sending a small (10–40 μamp) pulse of current for ½ sec in each direction, with a ½ sec open circuit period between pulses. The duration of the current was chosen to give resistance values after the rapid time-constant transients are over, but before any appreciable change has occurred in the long time-constant transient. A discussion of this problem has been presented elsewhere (Rehm, 1967). Current for the long time-constant transients was sent manually with the same device. Resistances are corrected for the resistance between the PD measuring electrodes (typically 28 Ω in our chamber).

RESULTS

In order to present a coherent set of figures, data in this paper were taken from a simple typical experiment in which all values were measured. While better fits have been obtained, this tissue, which was selected before a detailed fit was obtained, shows the general level of success of our method, and some of the problems involved. This particular tissue showed a H^+ secretory rate of 4.5 μeq/cm^2·hr, an open circuit PD of 20–22 mv (serosal positive; a negative PD in terms of the model), and a resistance of 167 Ω·cm^2. As seen in Fig. 3, the agreement between the calculated

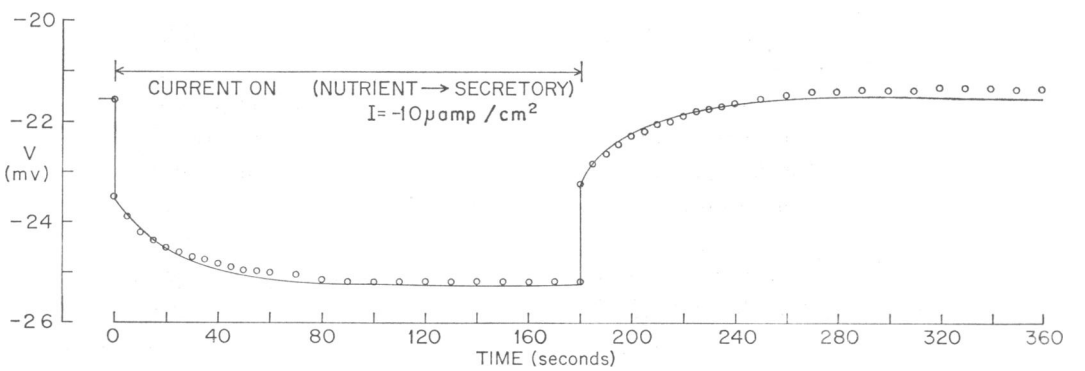

FIGURE 3 Comparison of model with frog gastric mucosa. Circles are points from experimental data; the lines are calculated from the model, using the following constants. Resistances (Ω·cm^2): R_1 = 4830, R_2 = 70, R_3 = 147, R_4 = 294. Volume = 3.2×10^{-7} 1/cm^2; C_0 = 0.1 M; E_1^A = −23.1 mv; I = −10 μamps/cm^2.

values and the measured ones is reasonably good at low current densities, and reasonable values are obtained for the various resistances and the cell volume.

The process of fitting the five available parameters is as follows.

(*a*) We already know the DC resistance of the tissue, $R_0 = 167\,\Omega\cdot\text{cm}^2$. Thus, only values of R's may be used which satisfy equation 2.

(*b*) From the work of Harris and Edelman (1964) as confirmed in this laboratory (Rehm, 1964; Spangler and Rehm, 1968), it appears that the K^+ conductivity of nutrient membrane is about twice the Cl^- conductivity, and that other ions have negligible conductivities. Using these two ions in our model, we thus require that $R_3 = R_4/2$. This restricts our choices in (*a*) above.

(*c*) From measurements on the tissue in question, we know V_∞. Subject to the above limitations, we must pick a set of values which will satisfy equation 10. For any ratio V_∞/V_0 (as determined experimentally), there are certain limits on the resistances we can choose, as shown in Fig. 4. For the present case, when $V_\infty/V_0 = 2.03$ and $R_0 = 167\,\Omega\cdot\text{cm}^2$, then R_2 must be less than $81\,\Omega\cdot\text{cm}^2$ to satisfy the equations. Since we are trying to pick reasonable and appropriate conditions for the real stomach mucosa, we feel that values of R_2 less than about $10\,\Omega\cdot\text{cm}^2$ are unreasonable. This still leaves a wide choice of values, all of which, in theory, will fit. However, the transient response is relatively stable; repetition of the current pulse will give the same transient, to a good approximation. We expect a certain variability in the conducitivity of any given path with time, and the observed constancy of the transient leads us to suspect that situations such as that represented by the curve $R_2 = 10\,\Omega\cdot\text{cm}^2$ in Fig. 4, are unrealistic, since very small changes in R_3 will cause large changes in V_∞/V_0 in the region of interest. It seems unlikely that R_3 is stable to better than 1% for periods of many hours, and our interest thus tends toward the left hand portion of Fig. 4, where the slope of V_∞/V_0 vs. R_3 is more gradual and R_2 is higher. These considerations aid us in reasonable choices for resistances. We have chosen, for this example, $R_2 = 70\,\Omega\cdot\text{cm}^2$, which fixes $R_3 = 147\,\Omega\cdot\text{cm}^2$ from Fig. 4, and $R_4 = 294\,\Omega\cdot\text{cm}^2$. R_1 is then calculated to be $4080\,\Omega\cdot\text{cm}^2$ by equation 2.

(*d*) We plot, for the real data, $\log |V_\infty - V|$ against time. The plot, for small current densities, approximates a straight line; i.e., it is an exponential function. Using the values for R's, and the ionic composition of the bathing solutions, we enter the computer program, and select a volume for compartment Y which satisfies the observed $\log |V_\infty - V|$ relationship.

(*e*) Finally, we can add the effect of active ion transport to the system. If we make the assumption that the observed PD across the tissue in the open circuit steady state is due to active transport of anion from the cell (Y) to the secretory bathing fluid (X), we replace the expression for E_2 by

$$E_2^A = E_2^0 + \frac{RT}{F} \ln \frac{[Cl]_X}{[Cl]_Y} = E_2^0 + E_2, \qquad (17)$$

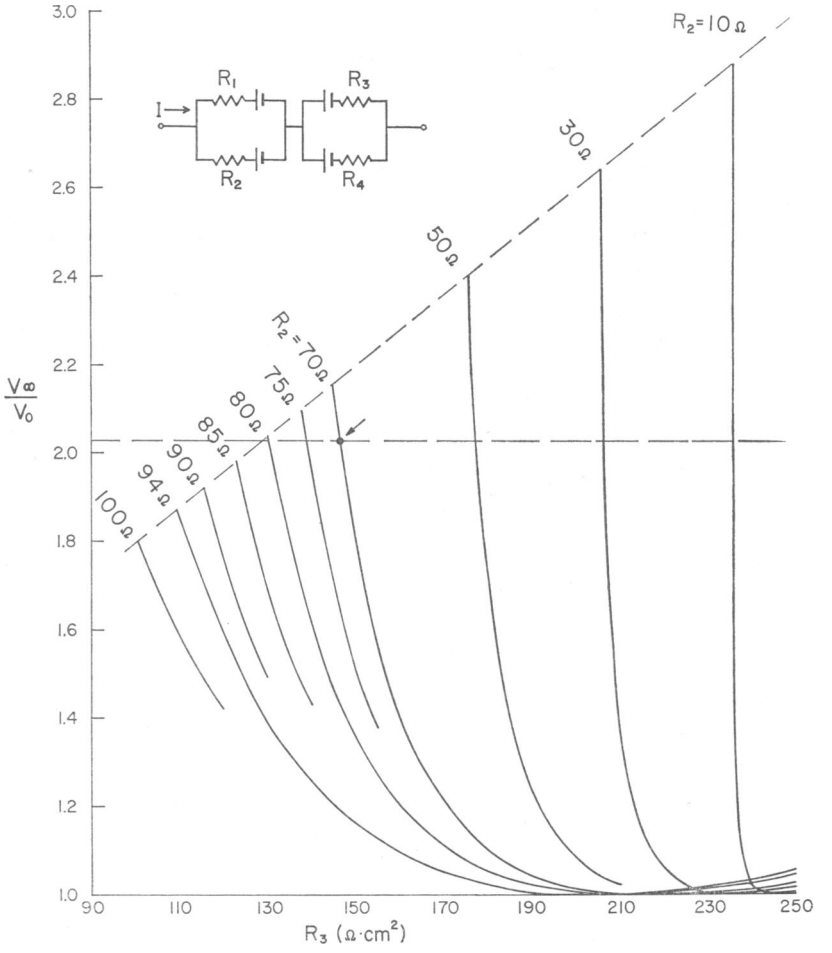

FIGURE 4 Relationship between V_∞/V_0 and resistances. This is a graphical presentation of equation 11. For this graph, R_0 = 167 $\Omega \cdot cm^2$, and $R_4 = 2R_3$. Such a figure can be used to select appropriate resistance values from the large number of combinations which satisfy R_0. The horizontal dashed line indicates the V_∞/V_0 of 2.03 which was to be fit; the diagonal dashed line gives the maximum V_∞/V_0 for any given R_2, which occurs when $R_1 = \infty$. The point indicated by the arrow represents the values actually chosen (see Fig. 3), for reasons given in the text.

in which E_2^A can be shown to be the potential of an active electrogenic pump (Rehm, 1965). We must now allow the computer program to determine the value of $[Cl]_Y$ under open circuit conditions for each value of E_2^A selected, by running the program to steady state as before, but with $I = 0$. We now vary E_2^A until a fit is obtained.

By the method just described, the model system parameters can be adjusted to give a reasonable fit to the observed data. Note that the one high resistance value, R_1 = 4080 $\Omega \cdot cm^2$, corresponds to the relative K^+ resistance of the secretory mem-

brane, which has been shown to be high (Harris and Edelman, 1964). It will be recalled that we are disregarding the H^+ secretion in our present model.

DISCUSSION

Cell Volume Determination

As pointed out previously, the cell volume determination depends on the initial value of C_Y, which is determined by the concentrations C_X and C_Z. When $C_X = C_Z = 100$ mM (about the real Cl^- concentration in the secretory fluid) then $v = 3.2 \times 10^{-7}$ 1/cm², for our example. If the active cells of the tissues formed a flat sheet, 1 cm² in area and 10 μ thick, then the cell volume would be around 10^{-6} 1/cm², 3 times our fitted value.

However, the frog mucosa is not a flat sheet of cells, and the effect of the secretory pits and folds is to increase the surface area by some factor, r, above the gross measured area. However, such an increase will not invalidate the determination of v, since the volume calculated from the model per unit gross area remains the same. The factor relating gross to actual area has not been measured in frog stomach, although it is about 13 for dog gastric mucosa (Canosa and Rehm, 1958). An approximate value might be $r = 5$, in which case if the cells were 10 μ thick, their collective volume for a gross area of 1 cm² would be 5×10^{-6} liters, or 15 times the value which satisfies the model. However, if $C_X = C_Z = 4$ mM (the K^+ concentration in Ringer's solution), then the fitted volume is increased to 8×10^{-6} liters/cm², a more reasonable fit to the calculated 5×10^{-6} liters/cm² from geometric considerations.

For small currents, we can use the results of Appendix B, which allows us to have unequal anion and cation concentrations, in conformity to the real situation. Comparing equation 14 with the exponent in equation 13 B, in Appendix B, shows that the difference resides in the concentration terms, and equation 14 will yield the same results as equation 13 B if an effective concentration, C_0', is defined, such that $C_0' = 2A_0B_0/(A_0 + B_0)$. In the present case, where $A_0 = 0.004$ and $B_0 = 0.1$ (molar), then $C_0' = 0.0077$ (molar) and the calculated volume is 4.16×10^{-6} liters/cm², which is still a reasonable fit. This technique is, of course, limited to currents sufficiently low that equation 13 B applies.

This fit, while satisfactory, may be fortuitous. We are in doubt as to the value of r and the thickness of the cell layer, and uncertainties as to the relative contributions of surface epithelial cells and pit cells, and uncertainties as to current distribution in invaginated systems (Rehm, 1968 *b*) make volume calculations tenuous. At any rate, our calculated volume is not at wide variance with values approximated in other ways, and the calculated resistance values are quite satisfactory.

Prediction of the Ba^{++} Effect

The addition of 0.1 mM $BaCl_2$ to the nutrient side of the frog gastric mucosa has been shown (Jacobson, Schwartz, and Rehm, 1965; Schwartz, MacKrell, Jacobson,

and Rehm, 1966; Schwartz, Pacifico, MacKrell, Jacobsen, and Rehm, 1968) to result in a large increase in the transmural resistance, without, however, markedly changing the acid secretory rate or potential difference. It appears that the primary action of Ba^{++} is to reversibly decrease the permeability of the nutrient membrane to K^+ (Pacifico and Rehm, 1967; Rehm, 1967; Sachs and Pacifico, 1968; Pacifico, Schwartz, MacKrell, Spangler, Sanders, and Rehm, 1969). The magnitude of the long time-constant transient is also greatly reduced (Rehm, 1967), an observation consistent with our model. The magnitude of the transient, V_∞/V_0, is determined by the asymmetry in the ratios of resistances R_2/R_1 to R_4/R_3, and it can be seen from equation 9 that if $R_2/R_1 = R_4/R_3$, there will be no transient. Since R_1 (the K^+ resistance of the secretory membrane) is normally high, an increase in R_3 (the K^+ resistance of the nutrient membrane) cause by Ba^{++} will tend to equalize the resistance ratio, and thus reduce the magnitude of the transient, at the same time increasing R_0. Both of these effects are observed. The model also predicts an increase in the time constant (decrease in θ) with an increase in the value of R_3 caused by Ba^{++}. Some of the records suggest that this may occur; however the experiments were not conducted with this in mind, and the very small residual transient is difficult to analyze with any accuracy.

Effects of High Current

In the computer solution there is no restriction on the value of I which may be used, and the theoretical effects of large currents can be investigated. Using the same constants as before, the expected curves for $I = 100$ μamp were plotted, and are compared with the 100 μamp curves for this tissue in Fig. 5. The fit is reasonable, but not as exact as before. As can be seen in Fig. 6, the transient is no longer a single exponential function, but has pronounced curvature, and differs for charge and discharge. Some of this behavior is predictable from the single-term analytical solution (equations 13–15) since the value of the exponential in equation 14 differs

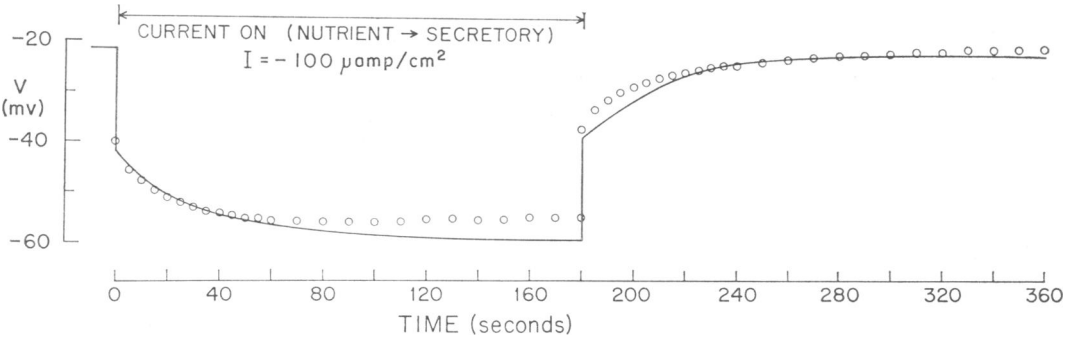

FIGURE 5 Comparison of the model with frog mucosa. Same tissue and parameters as Fig. 3, but $I = -100$ μamp/cm². For experimental data, V_∞ is taken as the value at maximum excursion.

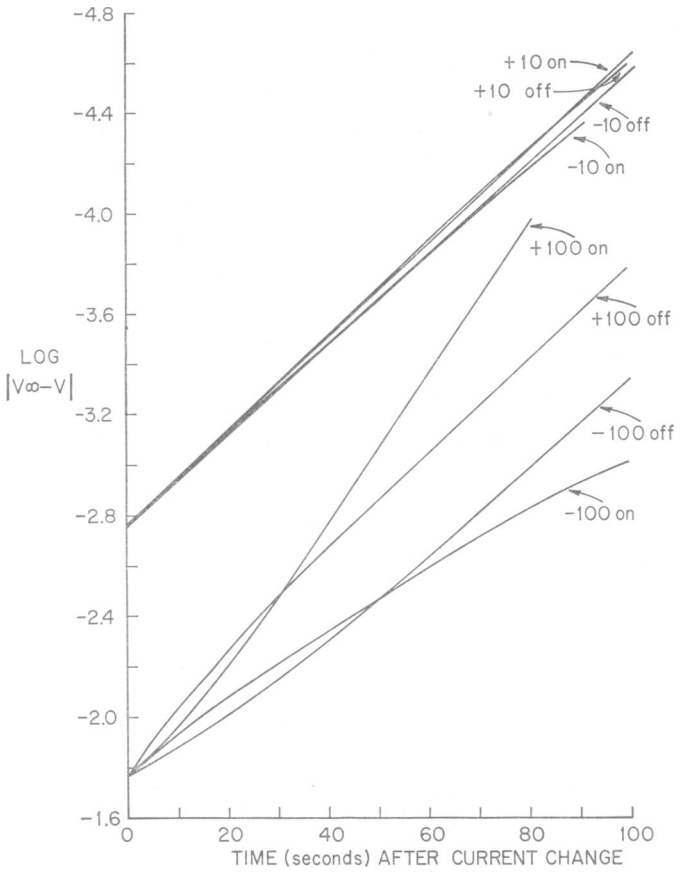

FIGURE 6 Calculated values (computer) for 10 and 100 μamp/cm^2 pulses, using the constants given in Fig. 3. Note the close approximation to a single exponential at 10 μamp, but considerable departures at 100 μamp/cm^2. The difference between these two groups at zero time is due to the difference in V_0 for the two current strengths.

from 1 at high current densities, which leads to values of θ greater for positive I and less for negative I than the $I = 0$ value. This is observed in the pseudoexponential parts of the curves, but is complicated by the curvature of the lines, which is not predicted by the single term simplification in equations 13 and 14.

Cell Concentration Changes

The physical basis for the changes in time constant and curvature with high current densities resides in the changes in intercellular concentration, C_Y, which leads to effects on the membrane potentials which are not symmetrical. Fig. 7 shows a set of computed concentration changes for two current densities. At 10 μamp/cm^2, the changes in cell concentrations are small, while at higher currents the changes are

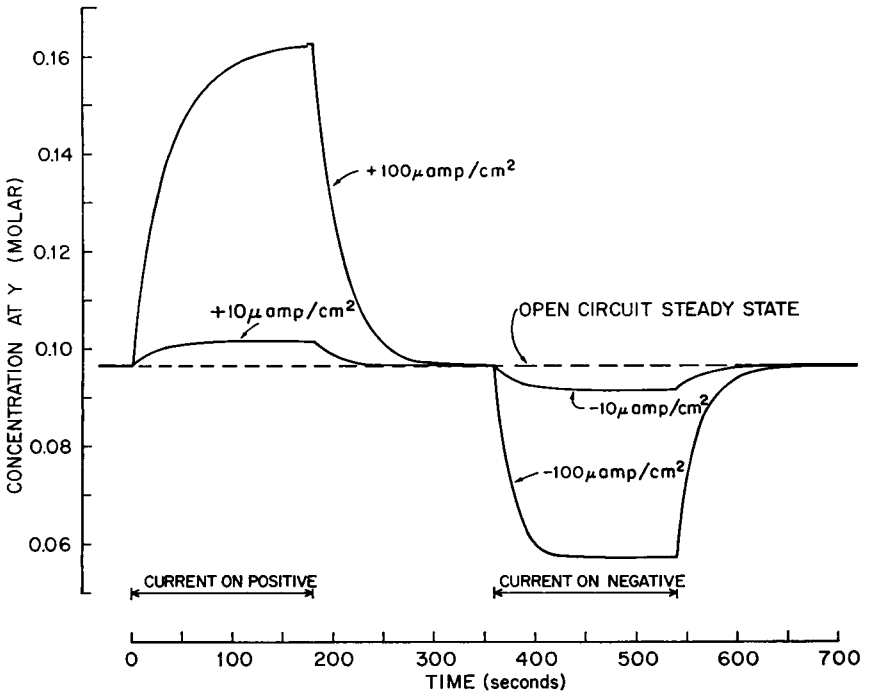

FIGURE 7 Calculated concentration change in the intercellular compartment (Y) at two current densities. Constants for the model same as in Fig. 3. Note the lack of symmetry at high current. External concentration 0.1 M, active transport component E_2^0 is −23.1 mv, oriented to transport Cl^- from Y to X.

considerable. Note that the changes are not reciprocal at high currents; in particular, negative 100 μamp current causes the concentration to reach to its steady state more quickly than for the positive 100 μamp current. This is not surprising, since the steady state is determined by concentration ratios, and more ions must be moved to effect a given ratio change in the direction of concentration increase than for a decrease. The 100 μamp/cm² current is not "unphysiological" for frog stomach, being about the value of the short-circuit current. Even at this level there is considerable concentration change, and thus there are departures from the strict exponential response.

Problems with the Model

Unfortunately for the model builder, living systems are not static. They respond to changes in their internal and external environment in a manner which is generally to oppose these changes. Several such responses, both active (homeostatic mechanisms) and passive changes, tend to alter the conditions of the system during the passage of current. While the good fit obtained at low currents shows that these effects are not serious under these conditions, at higher currents some, or all of these effects, should be included in a more comprehensive model.

Spontaneous PD variation with time is observed in all epithelial tissues. This variation tends to cause poor fit, since the model can have only one open circuit PD for a given set of conditions. We generally used pulse lengths of 180–200 sec, with the same period allowed for recovery, so the total experiment requires about 12 min for a complete set of pulses at one current. During this time, the spontaneous open circuit PD frequently changes. One cannot reduce the pulse length, however, without introducing other complications, since this system, in common with real *RC* circuits, shows nonsymmetrical charge-discharge curves if not allowed to charge to the steady state.

A second complication arises due to the self-regulating nature of biological systems. The cells of which we are speaking presumably have not only "transmural" active transport properties, but "homeostatic" active transport as well. The response of a cell to some condition which lowers its internal ion content would be expected to be an increase in homeostatic active transport in the compensatory direction. If we envision active pumps in electrogenic terms, this change in activity of the pumps could be either a change in the membrane resistance, or a change in the electrical pump potential, or both. In the present case we cannot say if the pump potential has changed, but we have some evidence that some membrane resistance does change at high currents, which would alter the predicted response.

We have measured the pulse resistance, R_0, during the course of a transient by superimposing on the transient current a small pulse step of current from another generator and measuring the voltage response as before. The length of the pulse current was 0.5 sec, which is sufficiently short that the error due to the long time-constant transient is only about 1 % at any time. The pulse is followed by another in the reversed polarity, to avoid changing the steady-state PD. The DC resistance, R_0 (as measured by this pulse method), can be shown to be nearly constant throughout a low current transient. At high currents, however, there is a marked change in R_0 as shown in Fig. 8. This change undoubtedly explains a part of our failure to obtain exact fit at high currents. It should be stressed that these resistance changes are not sufficient to explain the transient response. Indeed, at very low currents, the resistance change is below our ability to measure it, while the transient response, expressed as V_∞/V_0, is unaltered.

Another difficulty with this model is the dependence upon a single uni-univalent electrolyte, as mentioned above. Even granted that K^+ and Cl^- seem to be the major charge-carrying ions in the frog stomach system, the fact that we consider no other ions restricts our choices of solution concentrations to nonphysiological conditions. Ringer's solution has $K^+ = 4$ mM, while Cl^- 80 mM; our model requires that these be equal except in one special case. Nor is it possible to rig the experimental condition to fit the model, as both high K^+ (Davis, Rutledge, Keesee, Bajandas, and Rehm, 1965; Rehm, Sanders, Rutledge, Davis, Kurfess, Keesee, and Bajandas, 1966) and low total ionic composition (Sanders and Rehm, 1968) have been shown to change the tissue resistance. Indeed, the critical concentration, C_Y,

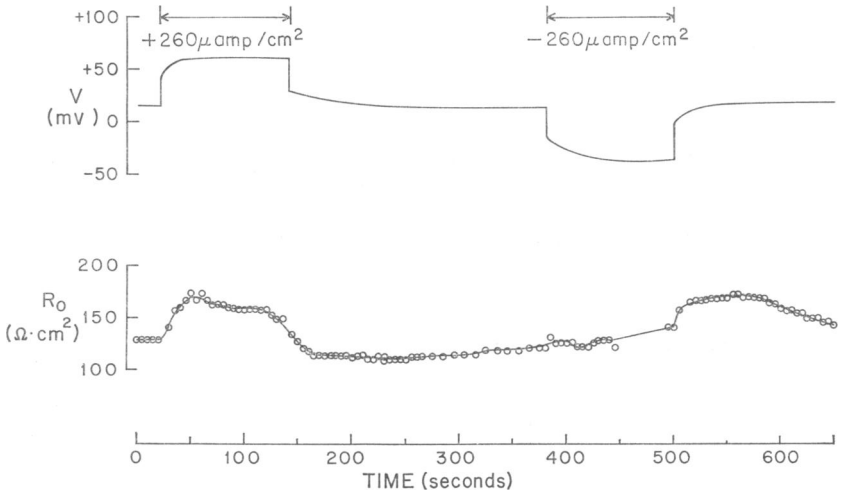

FIGURE 8 Tissue resistance (R_0) as measured by ½-sec current pulse superimposed on a long time-constant transient at high current density. Note rapid R_0 changes associated with positive current steps, whether these are changes from 0 to +, or from − to 0. Negative current steps give slower changes. R_0 is a constant at low current densities.

is not accessible to much experimental manipulation since homeostatic active transport mechanisms presumably control the cellular composition, and we are not even certain of the cellular concentration of major ions under normal conditions.

Nor have we considered the probable changes in intracellular volume which should accompany any changes in ionic composition. If the tonicity of the cells is appreciably altered by current passage, as it may be at high currents (Fig. 7), the cell volume should respond osmotically. Since cell volume is a part of our model and affects the calculated time constant, we would expect any such volume changes during a transient to cause errors.

Our model assumes that the major current carrier is a univalent electrolyte, presumably KCl. However, a considerable current is, in fact, carried by H^+ across the secretory membrane. Likewise, we have not considered ion movements which do not involve net charge transfer, such as ion pair migration or Cl^-/HCO_3^- exchange, which may well exist.

Other Possible Models

The model proposed is not the only way in which a concentration change can give rise to a polarization emf across a membrane system. One other mechanism is worth consideration. There are unstirred layers of appreciable thickness on each side of the frog mucosa, formed on the nutrient side by the connective tissue layer and the muscularis mucosae, and on the mucosal surface by the trapped fluid in the pits and the mucous coat. If we imagine a membrane more permeable to cations

than anions adjacent to such an unstirred layer, passage of current across this system can cause changes in ion composition in the unstirred layer, leading to diffusion emf changes, and consequent transient behavior. It is not the purpose of this paper to develop this model system, but its existence should be recognized, as there is some data to indicate that it may be a factor under certain circumstances (Noyes, unpublished observations).

In view of these complexities, it is surprising that the model gives as good a fit as it does. The objections are not, apparently, sufficiently serious to invalidate the model. The reasonable fit gives us some confidence that the principles underlying this model are sound, and that further work is justified.

Many of these difficulties can be overcome by a more complex, "second generation," model, which includes conductivities for several anions and cations, allows the use of physiological concentrations in the model, and allows for active H^+ transport. Such a model is under construction, and appears to be usable, but its evaluation is beyond the scope of the present paper.

CONCLUSIONS

We hope to have demonstrated: (*a*) that a model system consisting of two membranes enclosing an (intracellular) volume can give a voltage response which fits the observed long time-constant transient without requiring large values of membrane capacitance, (*b*) that such a model predicts the observed exponential rise and decay times at low current densities, and departures from exponential behavior at high currents, (*c*) that such effects as the abolition of the transient by Ba^{++} are consistent with the model, (*d*) that the values for resistances and intercellular volume calculated on this basis are reasonable ones, consistent with values determined in other ways, (*e*) that these considerations severely restrict the values of resistances which represent the various membrane ion conductivities, and (*f*) that in a two-membrane system, the evaluation of the parameters of the individual membranes is aided by the restrictions on possible resistance values imposed by this model.

APPENDIX A

The purpose of this section is to develop the equation expressing V as a function of time, of which equations 12 and 13 are the first term. To keep the expressions manageable, we will combine constants liberally; for these, see Glossary.

Solving equation 9 for ΔV, using equations 3, 8, and the glossary terms, one obtains

$$\Delta V = V - V_0 = -\frac{2BE}{a}. \qquad (1\text{ A})$$

Solving equation 7 for C_Y, differentiating both it and (1 A) with respect to time, combining and rearranging yields

$$\frac{dC_Y}{dt} = \frac{-aC_0 e^{-\gamma\Delta V}}{2hB}\,\frac{d\Delta V}{dt}. \qquad (2\text{ A})$$

Another expression for dC_Y/dt can be obtained by combining equations 4, 5, 8, 12, and 1 A, recalling that $I = I_1 + I_2 = I_3 + I_4$. This yields

$$\frac{dC_Y}{dt} = \frac{a\Sigma R_i \Delta V - B^2 I}{FvaB}. \tag{3 A}$$

Eliminating $(dC_Y)/(dt)$ between equations 2 A and 3 A and rearranging yields

$$\frac{d\Delta V}{dt} = \left[\frac{2hB^2 I - 2ha\Sigma R_i \Delta V}{FvC_0 a^2}\right] e^{\gamma \Delta V}. \tag{4 A}$$

Rearranging equation 4 A gives

$$\frac{d\Delta V}{[2hB^2 I - 2ha\Sigma R_i \Delta V]e^{\gamma \Delta V}} = \frac{dt}{FvC_0 a^2}. \tag{5 A}$$

This expression is an exponential integral for which a solution is available in standard tables. This is

$$\ln [B^2 I - a\Sigma R_i \Delta V] + \sum_{n=1}^{\infty} \frac{(PI - \gamma \Delta V)^n}{n \cdot n!} = \frac{-Ate^{PI}}{vC_0} + C_{\text{int}}. \tag{6 A}$$

When $t = 0$, $\Delta V = 0$,

$$C_{\text{int}} = \ln (B^2 I) + \sum_{n=1}^{\infty} \frac{(PI)^n}{n \cdot n!}, \tag{7 A}$$

which, when substituted for C_{int} in equation 6 A gives, after rearranging,

$$\Delta V = \Delta V_\infty \left\{1 - \exp\left[-\frac{Ate^{PI}}{vC_0} + \sum_{n=1}^{n} \frac{(PI)^n - (PI - \Delta V)^n}{n \cdot n!}\right]\right\}. \tag{8 A}$$

For discharge (when I is reduced to zero), when $t = 0$, $\Delta V_D = \Delta V_0$. Then

$$C_{\text{int}} = \ln (-a\Sigma R_i \Delta V_0) + \sum_{n=1}^{\infty} \frac{(-\gamma \Delta V_0)^n}{n \cdot n!} \tag{9 A}$$

and

$$\Delta V_D = \Delta V_0 \exp\left[-\frac{At}{vC_0} + \sum_{n=1}^{\infty} \frac{(-\gamma \Delta V_0)^n - (-\gamma \Delta V_D)^n}{n \cdot n!}\right]. \tag{10 A}$$

If the system had reached a steady state during charging (current on), then, at the time the current was turned off, $\Delta V_0 = \Delta V_\infty$. Otherwise, ΔV_0 is equal to ΔV of equation 8 A. The infinite series in equations 8 A and 10 A will be different for $+I$ and $-I$. This follows since when I is positive, ΔV_0 and ΔV_∞ are positive and vice versa. Furthermore, the system is not bilaterally symmetrical, i.e., the response to $+I$ will not be superimposable on the inverse of the response to $-I$, unless I is very small. The physical significance of this assymmetrical behavior is discussed in the text.

APPENDIX B

The purpose of this section is to develop an equation for expressing V as a function of time when the concentration of the permeant cation and anion are different. In this modification

of the model, it is still assumed that the membranes are permeable to only one cation and one anion so that the model illustrated by the circuit in Fig. 2 is still applicable. However, we introduce nonpermeant ions in the bathing solution and in the "cell" between the membranes.

In compartment Y the concentration of cation is given by

$$B_Y = B_0 + \Delta C \tag{1 B}$$

and that of the anion by

$$A_Y = A_0 + \Delta C, \tag{2 B}$$

where B_0 and A_0 are the initial concentrations in compartment Y and are the concentrations in the bathing fluids at X and Z at all times. B_0 may be larger than, equal to, or less than A_0. ΔC represents the change in concentration of the permeant cation (and also the permeant anion) in region Y following the application of current.

At all times

$$E_1 = -E_3 \quad \text{and} \quad E_2 = -E_4, \tag{3 B}$$

from which it follows that (by subtraction)

$$\Delta E = E_1 - E_2 = -(E_3 - E_4). \tag{4 B}$$

Combining equations 3–6, 3 B, and 4 B we have

$$V - V_0 = \Delta V = -\frac{B}{a}\Delta E. \tag{5 B}$$

The E's are given by the Nernst equation

$$\Delta E = E_1 - E_2 = -E_3 + E_4 = h \ln\left(\frac{B_0 + \Delta C}{B_0}\right) + h \ln\left(\frac{A_0 + \Delta C}{A_0}\right). \tag{6 B}$$

We will assume that $\ln (1 + x) = x$ so that equation 6 B reduces to

$$\Delta C = \frac{A_0 B_0 \Delta E}{h(A_0 + B_0)}, \tag{7 B}$$

and eliminating ΔE from equation 7 B by equation 5 B gives

$$\Delta C = \frac{aA_0 B_0 \Delta V}{hB(A_0 + B_0)}, \tag{8 B}$$

and differentiating equation 8 B with respect to time yields

$$\frac{d\Delta C}{dt} = \frac{-aA_0 B_0}{hB(A_0 + B_0)} \cdot \frac{d\Delta V}{dt}. \tag{9 B}$$

Combining equations 3–5, 12, and 4 B gives

$$\frac{d\Delta C}{dt} = -\frac{\Sigma R_i \Delta E + BI}{Fva}, \qquad (10\ B)$$

and using equation 5 B we have

$$\frac{d\Delta C}{dt} = \frac{a\Sigma R_i \Delta V - B^2 I}{FvaB}. \qquad (11\ B)$$

Eliminating $(d\Delta C)/(dt)$ from equations 9 B and 11 B yields

$$\frac{d\Delta V}{dt} = \frac{(-a\Sigma R_i \Delta V + B^2 I)h(A_0 + B_0)}{Fva^2 A_0 B_0}. \qquad (12\ B)$$

Integration and evaluating the constant of integration for $\Delta V = 0$ and $t = 0$ gives

$$\Delta V = \Delta V_\infty \left\{1 - \exp\left[\frac{-h\Sigma R_i (A_0 + B_0)t}{FvaA_0B_0}\right]\right\}. \qquad (13\ B)$$

This equation reduces to equation 13 when $A_0 = B_0 = C_0$ and when the exponential term in equation 14 is given a value of unity (low current case).

Evaluating the constant of integration for $\Delta V_D = \Delta V_0$, $I = 0$ and $t = 0$ yields

$$\Delta V_D = \Delta V_0 \exp\left[\frac{-h\Sigma R_i (A_0 + B_0)t}{FvaA_0B_0}\right] \qquad (14\ B)$$

which reduces to equation 15 when $A_0 = B_0 = C_0$.

GLOSSARY FOR APPENDIX A AND B

$B = R_1R_4 - R_2R_3$
$a = (R_1 + R_2)(R_3 + R_4)$
$h = RT/ZF$
$C_0 = C_X = C_Z =$ concentration at X and Z
$\gamma = a/2hB$
$\Sigma R_i = R_1 + R_2 + R_3 + R_4$
$\Delta V_\infty = V_\infty - V_0 = B^2I/a\Sigma R_i$
$A = 2h\Sigma R_i/Fa$
$P = B/2h\Sigma R_i$
$C_{int} =$ integration constant

Supported by NSF GN-6927X and NIH R01-NB08313. Part of this work was performed during the tenure of a U.S.P.H.S. Special Postdoctoral Fellowship (1-F3-GM-8718-01) to Dr. Kidder.

Received for publication 23 May 1968 and in revised form 28 July 1969.

REFERENCES

CANOSA, C. A., and W. S. REHM. 1958. *Gastroenterology.* **35**:292.
COOPERSTEIN, I. L., and C. A. M. HOGBEN. 1959. *J. Gen. Physiol.* **42**:461.

CRANE, E. E., and R. E. DAVIES. 1951. *Biochem. J.* **49**:169.
CRANE, E. E., R. E. DAVIES, and N. M. LONGMUIR. 1948. *Biochem. J.* **43**:336.
CURRAN, P. F., and M. CEREIJIDO. 1965. *J. Gen. Physiol.* **48**:1011.
DAVIS, T. L., J. R. RUTLEDGE, D. C. KEESEE, F. J. BAJANDAS, and W. S. REHM. 1965. *Amer. J. Physiol.* **209**:146.
DURBIN, R. P., and E. HEINZ. 1958. *J. Gen. Physiol.* **41**:1035.
FINKELSTEIN, A., and A. MAURO. 1963. *Biophys. J.* **3**:215.
HARRIS, J. B., and I. S. EDELMAN. 1964. *Amer. J. Physiol.* **206**:769.
HOGBEN, C. A. M. 1955. *Amer. J. Physiol.* **180**:641.
JACOBSON, A., M. SCHWARTZ, and W. S. REHM. 1965. *Physiologist.* **8**:200.
MAURO, A. 1961. *Biophys. J.* **1**:353.
PACIFICO, A. D., and W. S. REHM. 1967. *Physiologist.* **10**:271.
PACIFICO, A. D., M. SCHWARTZ, T. N. MACKRELL, S. G. SPANGLER, S. S. SANDERS, and W. S. REHM. 1969. *Amer. J. Physiol.* **216**:536.
SACHS, G., and A. PACIFICO. 1968. *Fed. Proc.* **27**:748.
SANDERS, S. S., and W. S. REHM. 1968. Abstracts of the Biophysical Society 12th Annual Meeting. Biophysical Society, New York. A 171.
SCHWARTZ, M., T. N. MACKRELL, A. JACOBSON, and W. S. REHM. 1966. *Physiologist.* **9**:284.
SCHWARTZ, M., A. D. PACIFICO, T. N. MACKRELL, A. JACOBSON, and W. S. REHM. 1968. *Proc. Soc. Expt. Biol. Med.* **127**:223.
SPANGLER, S. G., and W. S. REHM. 1968. *Biophys. J.* **8**:1211.
REHM, W. S. 1943. *Amer. J. Physiol.* **139**:1.
REHM, W. S. 1945. *Amer. J. Physiol.* **144**:115.
REHM, W. S. 1950. *Gastroenterology.* **14**:401.
REHM, W. S. 1953. *Amer. J. Physiol.* **172**:689.
REHM, W. S. 1956. *Amer. J. Physiol.* **185**:325.
REHM, W. S. 1962 *a*. *Amer. J. Physiol.* **203**:63.
REHM, W. S. 1962 *b*. *Amer. J. Physiol.* **203**:1091.
REHM, W. S. 1964. Abstracts of the Biophysical Society 8th Annual Meeting. Biophysical Society, New York.
REHM, W. S. 1965. *Fed. Proc.* **24**:1387.
REHM, W. S. 1967. *Fed. Proc.* **26**:1303.
REHM, W. S. 1968 *a*. Abstracts of the Biophysical Society 12th Annual Meeting. Biophysical Society, New York. A18.
REHM, W. S. 1968 *b*. *J. Theoret. Biol.* **20**:341.
REHM, W. S., S. S. SANDERS, J. R. RUTLEDGE, T. L. DAVIS, J. F. KURFESS, D. C. KEESEE, and F. J BAJANDAS. 1966. *Amer. J. Physiol.* **210**:689.
USSING, H. H., and E. E. WINDHAGER. 1964. *Acta Physiol. Scand.* **61**:484.
USSING, H. H., and K. ZERAHN. 1951. *Acta Physiol. Scand.* **23**:110.